Magnetic Dichroism in *K*-Shell Photoemission from Laser Excited Li Atoms

M. Meyer,[1,2] A. N. Grum-Grzhimailo,[3] D. Cubaynes,[2] Z. Felfli,[4] E. Heinecke,[5,6] S. T. Manson,[7] and P. Zimmermann[6]

[1]*European XFEL GmbH, Albert-Einstein-Ring 19, D-22761 Hamburg, Germany*
[2]*Institut des Sciences Moléculaires d'Orsay, Centre Universitaire Paris-Sud, Bâtiment 350, F-91405 Orsay Cedex, France*
[3]*Institute of Nuclear Physics, Moscow State University, Moscow 119991, Russia*
[4]*Centre for Theoretical Studies of Physical Systems, Clark Atlanta University, Atlanta, Georgia 30314, USA*
[5]*Institut für Experimentalphysik, Freie Universität Berlin, Arnimallee 14, D-14195 Berlin, Germany*
[6]*Institut für Optik und Atomare Physik, Technische Universität Berlin, Hardenbergstrasse 36, D-10623 Berlin, Germany*
[7]*Department of Physics and Astronomy, Georgia State University, Atlanta, Georgia 30303, USA*

(Received 15 August 2011; published 14 November 2011)

Magnetic dichroism in the angular distribution has been demonstrated for single-electron photoemission from inner ns^2 subshells of gaseous atomic targets using the example of *K*-shell photoionization of polarized Li atoms laser prepared in the $1s^2 2p\ ^2P_{3/2}$ excited state. The effect is pronounced for the conjugate shakeup and conjugate shakedown photoelectron lines, and less important, though observable, for the main and direct shakeup lines. The phenomenon is caused by configuration interaction in the final continuum state and is quantitatively described by the close-coupling *R*-matrix calculations.

DOI: 10.1103/PhysRevLett.107.213001 PACS numbers: 32.80.Fb, 32.80.Aa

Photoemission from anisotropic targets, such as polarized atoms, oriented molecules, magnetized films and 2D materials, generally depends on the target orientation with respect to the polarization vector of the incoming radiation. The difference of the photoelectron flux for two target polarizations is quantified by various kinds of magnetic dichroism in photoemission (MDPE). The MDPE in the extreme ultraviolet range, both angle-resolved and angle-integrated photoemission, accompanied by remarkable theoretical developments, provides valuable information on electron structure and bonding [1], element-resolved magnetic structure [2] and, more generally, on the origin and dynamics of magnetic phenomena [3]. In atomic photoionization, the MDPE serves as a basis for the ''perfect'' experiment, aimed at complete quantum mechanical knowledge of the process (e.g., [4,5]). However, in atomic single photoionization from closed *s* subshells, the MDPE is normally expected to be negligible, since the emission of the spherically symmetric *s* electron should, in first approximation, not depend on the target polarization. It can even be shown explicitly [6] that in the single-configuration nonrelativistic approximation any kind of MDPE vanishes in the photoionization of an *s* electron.

In principle, the interaction of the ejected electron on its way through the atom with the charge cloud of the anisotropic valence shell can lead to a dependence of the photoelectron flux on the polarization state of the outer shell and generate MDPE in inner-shell ns^2 photoionization for isolated atoms. A similar mechanism works in molecules, when the angular distribution of *K*-shell photoemission crucially depends on the orientation of the molecule due to scattering of photoelectrons by the anisotropic potential of the residual molecular core [7]. However, recent measurements at the free electron laser FLASH in Hamburg (Germany) with laser-aligned $\mathrm{Li}^*(2p)$ atoms did not observe, within the statistical accuracy of 1%, alignment dependence of *K*-shell single ionization for photon energies of 85–91 eV [8]. Since in these experiments the residual ionic discrete Li^+ states were not resolved, the possible dichroic effect could have been smeared out and the general conclusion about negligible MDPE is doubtful. In addition, even in high-resolution experiments with combined laser and synchrotron radiation beams [9], no effects of the alignment of the laser-excited $\mathrm{Li}^*(2p)$ state on the *K*-shell ionization were noticed, because revealing of the dichroism was most likely prevented by low statistics.

This Letter reports on the first measurements and theoretical interpretation of the MDPE in atomic photoionization of a ns^2 subshell. For the experiments, we applied angle-resolved electron spectroscopy at the high-brilliance third generation synchrotron radiation (SR) source BESSY II (Berlin, Germany) and used laser optical pumping to produce excited $\mathrm{Li}^*(2p)$ atoms with variable polarization. The geometry of the setup is shown in Fig. 1. The counter-propagating laser and SR intersect a beam of lithium vapor, which is produced by a radiatively heated oven, in the source volume of a high-resolution electron energy analyzer (Scienta SES-2002) mounted at the magic angle (54°44′) with respect to the horizontal linear polarization vector of the SR. Both linearly and circularly polarized SR beams were used to measure at a fixed electron emission angle the linear magnetic dichroism in the angular distribution (LMDAD) and the circular magnetic dichroism in the angular distribution (CMDAD), respectively. The polarized Li atoms were produced via optical pumping of the Li $1s^2 2s\ ^2S_{1/2} - \mathrm{Li}^* 1s^2 2p\ ^2P_{3/2}$ transition at 671 nm with a narrow band (1 MHz) cw ring dye laser. In order to measure the magnetic dichroism in the *K*-shell

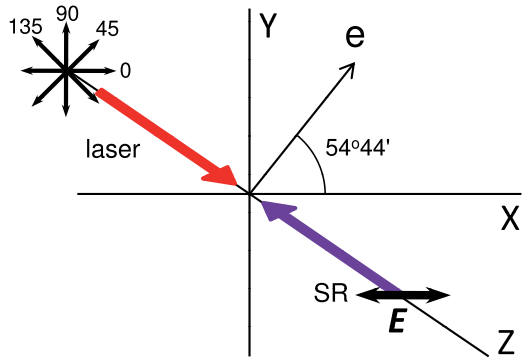

FIG. 1 (color online). Geometry of the setup with linearly polarized laser and linearly polarized SR for measurements of the LADAD(0/90) and LADAD(45/135). The LMDAD (CMDAD) is measured with circularly polarized laser in combination with linearly (circularly) polarized SR.

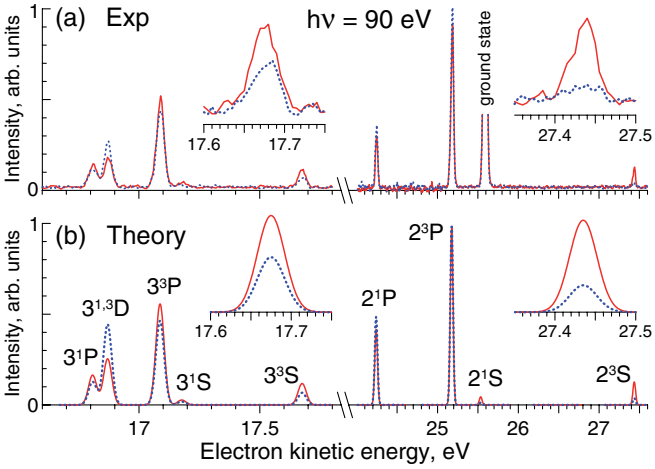

FIG. 2 (color online). Measured (a) and calculated (b) angle-resolved photoelectron K-shell spectra of Li initially in the oriented $1s^2 2p\ {}^2P_{3/2}$ state for two opposite orientations: Excitation with left- (right-) handed circularly polarized laser light is indicated by the blue-dotted (red-solid) line. The SR beam with the energy of 90 eV is linearly polarized and collinear with the atomic orientation. Insets show lines 3^3S and 2^3S in more detail. The maximal value of the orientation parameter [15] ($\mathcal{A}_{10} = 3/\sqrt{5}$) is implied in the theoretical calculations. The strong line at 25.6 eV in panel (a) corresponds to the photoionization of ground state atoms (see text).

photoionization, circularly polarized laser light was used, generating oriented Li atoms in the $^2P_{3/2}$ excited state. Changing the helicity of the laser by means of a rotatable quarter wave plate reverses the initial atomic polarization and enables us to determine the LMDAD and CMDAD as differences between the photoelectron intensities for left- and right-handed circularly polarized laser light. By combining both linearly polarized laser and SR, we observed the linear alignment dichroism in the angular distribution (LADAD), which is defined as the difference between the photoelectron intensities for the directions ϕ and $\phi + 90°$ of the laser polarization with respect to the electric field vector of the SR. The two independently measured quantities are LADAD(0/90) and LADAD(45/135) for $\phi = 0°$ and $\phi = 45°$, respectively, (Fig. 1). The overall resolution of the present experiment was set to 40 meV comprising both the bandwidth of the SR and the resolution of the electron analyzer. Electron spectra were recorded at photon energies of $h\nu = 85$, 90, 100, and 122 eV, i.e., away from the resonance regions where autoionizing states of Li are located [10]. The majority of measurements were performed with linearly polarized SR, since the CMDAD could only be measured at 122 eV due to undulator restrictions for producing circularly polarized SR at lower photon energies.

Figure 2(a) gives an example of two photoelectron spectra recorded for opposite directions of the $\mathrm{Li}^*(2p)$ orientation with linearly polarized SR at the photon energy of 90 eV. For the mutual normalization of the two measured spectra we used the fact that the MDPE from the Li ground state vanishes (see below). The closely lying ^1D and ^3D components of the $1s3d$ line, which are separated by only 4 meV, were not resolved in the experiment. The conjugate shakedown line $1s2s\,^1S$ located at 25.53 eV kinetic energy overlaps with the main $1s2s\,^3S$ line arising from photoionization of the remaining ground state atoms. Therefore, this line as well as the very weak $1s3s\,^1S$ line were excluded from the analysis. The LMDAD, which is the difference between the two spectra, is clearly much stronger than one would expect for an effect never observed before; for the conjugate shakeup into the $1s3s\ ^3S$, $1s3d\ ^{1,3}D$ states and conjugate shakedown into the $1s2s\ ^3S$ state the dichroism is of the same order of magnitude as the cross section itself. The LMDAD for the main lines $1s2p\ ^{1,3}P$ and the shakeup lines $1s3p\ ^{1,3}P$ is smaller, but still observable.

As noted above, in the nonrelativistic single-configuration approximation no MDPE is expected in atomic photoionization from ns^2 subshells. While the relativistic spin-orbit interaction in the final state was pointed out as a possible reason for a small ($\sim 0.1\%$) MDPE in photoionization from the $3s^2$ core subshell of ferromagnetic Fe [11], this mechanism cannot work for isolated light atoms like Li with negligible spin-orbit interactions. Therefore, configuration interaction must be accounted for to explain the experimental results. The large values of the observed MDPE for the conjugate shake transitions $2p \rightarrow ns, n'd$ already point to those configurations causing the main effect. Whereas the normal shake transitions lead to configurations of the residual ion with the same parity as the main line $1s2p$, the conjugate shake transitions are characterized by the opposite parity of the corresponding configurations $1sns, n'd$. Therefore the main ionization channel $\gamma + \mathrm{Li}^*(1s^2 2p) \rightarrow \mathrm{Li}^+(1s2p) + \epsilon p$, characterized by an emitted ϵp electron with kinetic energy ϵ, should be coupled to channels $\mathrm{Li}^+(1sns) + \epsilon s$, ϵd and

$Li^+(1sn'd) + \epsilon s$, ϵd, ϵg with emitted ϵs, ϵd, and ϵg electrons.

In first approximation, the normal shake process can be considered as the result of the sudden change of the potential due to the ejection of the $1s$ electron and the transition probability by the overlap (monopole) matrix elements $\langle 2p|np\rangle$ [12]. Similarly, the conjugate shake transitions can be represented in a simplified picture as $1s$ photoionization process $\gamma + Li^*(1s^2 2p)$ leading, for example, to the final ionic state $Li^+(1s3d)$ by a E1 transition $2p \rightarrow 3d$ accompanied by the $1s \rightarrow \epsilon s$ shakeoff. Such a picture based on simple overlap arguments is, however, quite insufficient to explain the observed phenomenon of MDPE. For the normal shake process, the $\langle 2p|np\rangle$ overlap is independent of the polarization of the $2p$ state; for the conjugate shake process, the $2p \rightarrow 3d$ transition induced by linearly polarized SR light is invariant with respect to reversing the sign of the magnetic quantum numbers of the $2p$ electron and, therefore, cannot produce any LMDAD. Moreover, the emitted ϵs photoelectron is isotropic, while the accurate R-matrix calculations predict high anisotropy of the photoelectrons in the conjugate shakeup into $Li^+(1s3d)$ [10]. Thus, even a qualitative description of the MDPE necessitates sophisticated methods, which include extensive configuration mixing and interchannel coupling [10,13], to account for the active $1s$ electron exchanging energy and orbital momentum with the $2p$ electron.

To express the MDPE in terms of the LS-coupled channel photoionization amplitudes, we use the theory developed in Refs. [6,14]. Neglecting relativistic effects and summing up over the unresolved final Li^+ fine-structure states, for the above geometry we obtain (in atomic units) for magnetic dichroism

$$\mathrm{LMDAD} = -\frac{\pi\alpha\omega}{3}\mathcal{A}_{10}\sqrt{\frac{5}{3}}\mathrm{Im}\bar{B}_{122}, \quad (1)$$

$$\mathrm{CMDAD} = -\frac{\pi\alpha\omega}{3}\mathcal{A}_{10}\frac{\sqrt{3}}{4}(\sqrt{2}\bar{B}_{101} + \bar{B}_{121}). \quad (2)$$

Here ω is the photon energy, α is the fine-structure constant and $\mathcal{A}_{10}$ is the orientation parameter of the initial Li $2^2P_{3/2}$ state [15], whose value depends on the laser pumping conditions. The maximal orientation is achieved when all the excited atoms are accumulated in a state with the maximal absolute magnetic quantum number $m = 3/2$ or $m = -3/2$. The LADAD(0/90) and LADAD(45/135) are expressed by Eq. (8) of [16] and are proportional to the alignment parameter $\mathcal{A}_{20}$ of the Li $2^2P_{3/2}$ state [15]. The dynamical parameters $\bar{B}_{k_0 k k_\gamma}$ are given by Eq. (32) of [6] (the bar indicates summation over the residual ion fine-structure levels). They are bilinear combinations of the dipole matrix elements for transitions from the multiconfiguration LS-coupled Li 2^2P state to the channel described asymptotically by the multiconfiguration Li^+ final state with orbital angular momentum L_f, spin S_f, parity p_f, and the various allowed total orbital angular momenta of the channel, the sum of the photoelectron ℓ and the total orbital angular momentum of the channel L_f, L ($\boldsymbol{L} = \boldsymbol{L}_f + \boldsymbol{\ell}$). The total spin $S = \frac{1}{2}$ and the parity $p = +1$ of the channel are fixed by the conservation laws. Here we perform close-coupling 29-term target R-matrix calculations of the dipole matrix elements similar to [10]. Note that after summation over the fine-structure states of the residual ion any kind of MDPE vanishes in the ionization from the oriented Li $2^2S_{1/2}$ ground state.

To describe the relative strength of the MDPE and relate it directly to the measured spectra, it is convenient to introduce the relative (normalized) dichroism as a dimensionless quantity $\overline{\mathrm{MDPE}} = 2(I_1 - I_2)/(I_1 + I_2)$, where I_1 and I_2 are the intensities of the detected photoelectron line for two different polarization states of the target atom, provided that other parameters of the experiment are kept fixed. This quantity compares the difference between two spectra with the average spectrum $(I_1 + I_2)/2$.

Figure 3 displays selected results for the relative dichroism as a function of the photon energy. The absolute values of $\overline{\mathrm{LMDAD}}$ and $\overline{\mathrm{LADAD}}(45/135)$ for the main $2^{1,3}P$ photoelectron lines and normal shake satellites $3^{1,3}P$ do

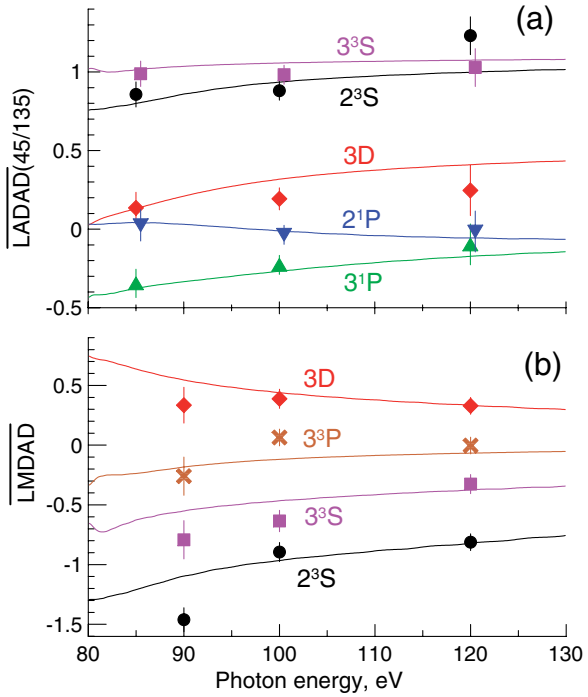

FIG. 3 (color online). $\overline{\mathrm{LADAD}}(45/135)$ (a) and $\overline{\mathrm{LMDAD}}$ (b) for ionization of $Li^* 1s^2 2p^2 P_{3/2}$ leaving the Li^+ ion in different $1sn\ell$ states. 3D denotes theory and experiment for unresolved 3^1D and ^3D states. Calculations are performed for the values $\mathcal{A}_{10} = 3/\sqrt{5}$, $\mathcal{A}_{20} = +1$ for $\overline{\mathrm{LMDAD}}$ (pumping with circularly polarized laser) and $\mathcal{A}_{20} = -1$ for the $\overline{\mathrm{LADAD}}$ (pumping with linearly polarized laser) [15].

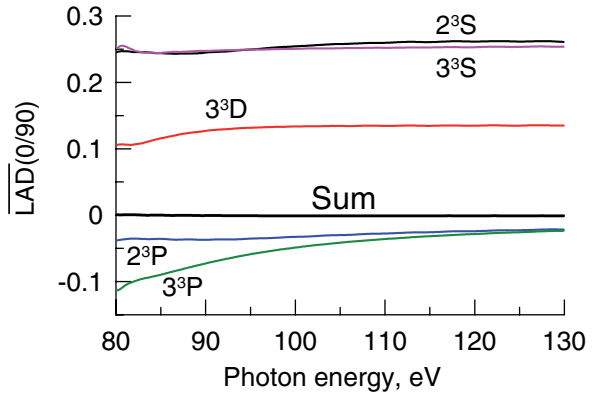

FIG. 4 (color online). Angle-integrated relative linear alignment dichroism $\overline{\mathrm{LAD}}(0/90)$ for the indicated Li^+ final states and the dichroism summed over ten states (see text).

not exceed ~0.4 both in experiment and theory [only one example is shown in Fig. 3(b)]. Furthermore, experiments recorded at 122 eV photon energy with circularly polarized SR did not show a measurable $\overline{\mathrm{CMDAD}}$ for any Li^+ state (not shown), in agreement with our calculations predicting very small absolute values, which do not exceed 0.15.

As it is seen from Figs. 2 and 3, the agreement between theory and experiment is generally very good, showing that our theoretical model correctly accounts for the main mechanisms producing the K-shell MDPE. The relative MDPE for the $2^{1,3}P$ and $3^{1,3}P$ lines is considerably smaller than for the conjugate shake transitions. This can be understood from the fact that in the former case the reason for the dichroism, i.e., the configuration mixing in the continuum, is only a small addition to the main mechanism producing the shakeup lines, while in the latter case the reason for the MDPE is the chief cause of the conjugate shake lines themselves. The relative importance of the configuration mixing in the continuum decreases with increasing photoelectron energy, thereby leading to smaller values of the MDPE for the $2^{1,3}P$ and $3^{1,3}P$ lines at higher photon energies. In addition, our interpretation is also in accordance with the observation of a large magnetic dichroism in the double photoionization of laser-excited Li at threshold and its decrease with increasing photon energy [8]. Considering the double photoionization as a combination of normal and conjugate shake processes (here for both electrons), these results are explained by large interchannel coupling and therefore high relative intensity of the conjugate shake process in the near threshold region.

A comment on the integral MDPE is appropriate here. Owing to symmetry reasons, in the angle-integrated photoelectron spectra linear magnetic dichroism LMD and linear alignment dichroism LAD(45/135) vanish for the individual lines, while circular magnetic dichroism CMD and linear alignment dichroism LAD(0/90) survive. The latter is shown in Fig. 4 for selected lines. Remarkably, after summing over the ten Li^+ $1s n\ell$ ($n\ell = 2s, 2p, 3s, 3p, 3d$) final states, the angle-integrated photoelectron fluxes for $\phi = 0°$ and $\phi = 90°$ become almost equal for photon energies 80–130 eV and $\overline{\mathrm{LAD}}(0/90)$ drops down to $\sim 10^{-3}$. This also explains nicely why due to the limited resolution no effect of the alignment of the $2p$ orbital was observed in [8] for the case of ionization with excitation. Such a compensation does not occur for the CMD; being summed over the same ten Li^+ final states, the calculated CMD shows values between −0.1 and −0.2 in the above range of photon energies.

In conclusion, by using the example of laser-excited Li in the $2p$ state, we observed magnetic dichroism in photoemission from atomic K shells. The effect is purely due to mixing of configurations in the atomic continuum and is explained theoretically by extensive close-coupling calculations.

We are grateful for the support of the BESSY staff during beam times and acknowledge funding by the European Community through the Research Infrastructure Action under the FP6 Structuring European Research Area Programme (contract R II 3-CT-2004-506008), NSF and DOE, Office of Chemical Sciences.

[1] W. Kuch and C. M. Schneider, Rep. Prog. Phys. **64**, 147 (2001).
[2] K. Starke, *Magnetic Dichroism in Core-Level Photoemission* (Springer, Berlin, 2000).
[3] J. Stöhr and H. C. Siegmann, *Magnetism. From Fundamentals to Nanoscale Dynamics* (Spinger, Berlin, 2006).
[4] O. Plotzke, G. Prümper, B. Zimmermann, U. Becker, and H. Kleinpoppen, Phys. Rev. Lett. **77**, 2642 (1996).
[5] K. Godehusen, P. Zimmermann, A. Verweyen, A. von dem Borne, Ph. Wernet, and B. Sonntag, Phys. Rev. A **58**, R3371 (1998).
[6] A. Verweyen, A. N. Grum-Grzhimailo, and N. M. Kabachnik, Phys. Rev. A **60**, 2076 (1999).
[7] F. Heiser, O. Geßner, J. Viefhaus, K. Wieliczek, R. Hentges, and U. Becker, Phys. Rev. Lett. **79**, 2435 (1997).
[8] G. Zhu *et al.*, Phys. Rev. Lett. **103**, 103008 (2009).
[9] D. Cubaynes, S. Diehl, F. J. Wuilleumier, M. Meyer, E. Heinecke, T. Richter, and P. Zimmermann, Phys. Rev. Lett. **99**, 213004 (2007).
[10] H. L. Zhou *et al.*, Phys. Rev. A **59**, 462 (1999).
[11] W. J. Lademan and L. E. Klebanoff, Phys. Rev. B **54**, 11725 (1996).
[12] Z. Felfli and S. T. Manson, Phys. Rev. Lett. **68**, 1687 (1992).
[13] G. B. Armen and F. P. Larkins, J. Phys. B **24**, 2675 (1991).
[14] S. Baier, A. N. Grum-Grzhimailo, and N. M. Kabachnik, J. Phys. B **27**, 3363 (1994).
[15] Orientation and alignment parameters of a state with the angular momentum $j = \frac{3}{2}$ are defined, respectively, as $\mathcal{A}_{10} = [3(N_{3/2} - N_{-(3/2)}) + (N_{1/2} - N_{-(1/2)})]/\sqrt{5}$ and $\mathcal{A}_{20} = (N_{3/2} + N_{-(3/2)}) - (N_{1/2} + N_{-(1/2)})$, where N_m is the relative population of magnetic substate with the projection m; $\sum_m N_m = 1$.
[16] D. Cubaynes *et al.*, Phys. Rev. A **80**, 023410 (2009).